DOI: 10.1002/ejic.200800415

Controlled Assembly of $[Nb_{6-x}W_xO_{19}]^{(8-x)-}$ (x = 0–4) Lindqvist Ions with (Amine)copper Complexes

Travis M. Anderson,[a] Mark A. Rodriguez,[a] Thomas A. Stewart,[a] Joel N. Bixler,[a] Wenqian Xu,[b] John B. Parise,[b] and May Nyman*[a]

Keywords: Niobium / Tungsten / Copper / Polyoxometalates

The mixed addenda isopolyanion, $[N(CH_3)_4]_2Na_2[$*cis*-$Nb_2W_4O_{19}]\cdot 18H_2O$, reacts with $Cu(NO_3)_2$ in water and in the presence of $NH_2CH_2CH_2NH_2$ (en) or NH_4OH at 60 °C to yield a phase that is decorated $\{[Cu(en)_2(H_2O)]_2[Nb_2W_4O_{19}]\cdot 2H_2O$ (**1**)$\}$ or charge-balanced $\{[Cu(NH_3)_4(H_2O)]_2[Nb_2W_4O_{19}]\cdot 8H_2O$ (**2**)$\}$, respectively, by (amine)copper complexes. The prolonged heating at 95 °C of $[N(CH_3)_4]_6[Nb_{10}O_{28}]\cdot 6H_2O$, $[N(CH_3)_4]_2Na_2[$*cis*-$Nb_2W_4O_{19}]\cdot 18H_2O$, or $Na_4K_2[$*cis*-$Nb_4W_2O_{19}]\cdot 12H_2O$ and $Cu(NO_3)_2$ in a mixed water/amine [en or $NH_2CH_2CH_2CH_2NH_2$ (dap)] solution results in the formation of two-dimensional materials with alternate layers of (amine)copper complexes linking Lindqvist $[Nb_{6-x}W_xO_{19}]^{(8-x)-}$ (x = 0–4) clusters. These phases include: $[Cu(dap)_2]_3[Nb_4W_2O_{19}]\cdot 7H_2O$ (**3**), $[Cu(dap)_2]_3[H_2Nb_6O_{19}]\cdot 6H_2O$ (**4**), $[Cu(dap)_2]_3[Nb_3W_3O_{19}]\cdot Cl\cdot 6H_2O$ (**5**), and $[Cu(en)_2]_3[Nb_4W_2O_{19}]\cdot 6H_2O$ (**6**). Complexes **4** and **5** result from the decomposition of $[Nb_{10}O_{28}]^{6-}$ and $[$*cis*-$Nb_2W_4O_{19}]^{4-}$ to $[H_2Nb_6O_{19}]^{6-}$ and $[$*fac*-$Nb_3W_3O_{19}]^{5-}$, respectively, in alkaline solution. Complex **5** contains an extra-framework site that is occupied by Cl^-, but this site is occupied by a water molecule in **3** and is vacant in structures **4** and **6**. The results of this study suggest that charge density, cluster charge and symmetry, and cluster-cation pairing are all important parameters in the incorporation of d-electron metals onto the surfaces of $[Nb_{6-x}W_xO_{19}]^{(8-x)-}$ (x = 0–4) clusters or into the frameworks of Lindqvist-based complex materials.

Introduction

Lindqvist's $[Nb_6O_{19}]^{8-}$ polyanion remains, since 1953, a cornerstone of isopolyniobate chemistry.[1–5] Synthetic and structural investigations of this cluster have produced transition-metal-decorated, linked, and protonated $[Nb_6O_{19}]^{8-}$ ions.[6–19] Salts of the $[Nb_6O_{19}]^{8-}$ ion have been crystallized with a variety of counter-cations including all of the alkali metals, as well as transition metal or lanthanide complexes.[1,9,11–14,16–22] Due to the high charge density of this cluster, it is stable only in alkaline solutions, and it is not readily dissolved or manipulated in non-aqueous media. These characteristics greatly limit the ability to incorporate d- and f-block elements into polyoxoniobate clusters or materials that are of considerable ongoing interest as proton conductors,[23] solid-state electrolytes (ion conductors),[24,25] catalysts,[26–29] and optical materials.[30]

The charge density of $[Nb_6O_{19}]^{8-}$ can be lowered by the substitution of one or more Nb^V addenda sites for W^{VI}, rendering the cluster less basic and more stable in neutral or acidic media. Dabbabi and Boyer reported that Na_2WO_4 and $K_8[Nb_6O_{19}]$ react in aqueous H_2O_2 to yield the mixed addenda complex $[NbW_5O_{19}]^{3-}$.[31] This compound is stable from pH = 1.5 to 5 and gradually transforms to $[$*cis*-$Nb_2W_4O_{19}]^{4-} \rightarrow [$*fac*-$Nb_3W_3O_{19}]^{5-} \rightarrow [$*cis*-$Nb_4W_2O_{19}]^{6-} \rightarrow [Nb_5WO_{19}]^{7-} \rightarrow [Nb_6O_{19}]^{8-}$ with increasing alkalinity. The isomeric purity of $[$*cis*-$Nb_2W_4O_{19}]^{4-}$, $[$*fac*-$Nb_3W_3O_{19}]^{5-}$, and $[$*cis*-$Nb_4W_2O_{19}]^{6-}$ was suggested by infrared studies[32] and further confirmed for $[$*cis*-$Nb_2W_4O_{19}]^{4-}$ by electrochemical measurements[33] as well as by ^{17}O and ^{183}W NMR spectroscopy.[34,35]

Recently, we investigated the reaction of $Rb_8[Nb_6O_{19}]$ and $Cu(NO_3)_2$ in a mixture of water and a coordinating amine designed to keep Cu^{II} soluble under the alkaline conditions necessary to stabilize $[Nb_6O_{19}]^{8-}$.[18] These studies produced a dimer with the formula $Rb_4[Cu(en)_2(H_2O)_2]_3[(H_2Nb_6O_{19})_2Cu(en)_2]$ and four one-dimensional solids consisting of alternating (amine)copper complexes and $[H_xNb_6O_{19}]^{(8-x)-}$ (x = 0, 2). The mixed-solvent/complex system also produced a new cluster type (based on $[Nb_7O_{22}]^{9-}$) that is derived from the Lindqvist ion.[36] Related studies were reported by Wang and co-workers, who found that the partial exchange of Na^+ with Ag^+ in $Na_7[HNb_6O_{19}]$ (or K^+ with Ba^{2+} in $K_7[HNb_6O_{19}]$), prior to the addition of a cupric salt, was crucial to the assembly of some of their new materials.[37] Collectively, these results suggest that the mixed-solvent/complex formulation, along

---

[a] Sandia National Laboratories,
Albuquerque, NM 87185, USA
E-mail: mdnyman@sandia.gov
[b] Department of Chemistry and Geosciences, SUNY – Stony Brook,
Stony Brook, NY 11794, USA

with appropriate consideration of ion pairing and charge density, may provide an avenue for further expansion of polyoxoniobate chemistry that should be more extensively explored.

We now report a synthetic and structural study of six new phases composed of Lindqvist ions and (amine)copper complexes. Five of these phases utilize the mixed addenda $[Nb_{6-x}W_xO_{19}]^{(8-x)-}$ (x = 2, 3, 4) clusters that are isostructural to $[Nb_6O_{19}]^{8-}$, but are more stable at lower pH values and can be more readily manipulated in non-aqueous solvent systems, because their charge densities are lower.[31,34] The sixth phase reported here uses the low-charge-density decaniobate cluster $[N(CH_3)_4]_6[Nb_{10}O_{28}]$ as an alkali-metal-free source of $[Nb_6O_{19}]^{8-}$ (by controlled hydrolysis) in order to further understand how ion pairing between alkali cations and $[Nb_6O_{19}]^{8-}$ affects the assembly of new cluster-based materials.[38,39] Each Lindqvist ion (or Lindqvist ion source in the case of $[N(CH_3)_4]_6[Nb_{10}O_{28}]$) was treated with $Cu(NO_3)_2$ in water and in the presence of NH_4OH, $NH_2CH_2CH_2NH_2$ (en), or $NH_2CH_2CH_2CH_2NH_2$ (dap). Crystallographic studies reveal that one phase is decorated by charge-balancing (amine)copper complexes $\{[Cu(en)_2(H_2O)]_2[Nb_2W_4O_{19}]\cdot 2H_2O$ (**1**)}, one phase has charge-balancing (amine)copper complexes that are completely unassociated with the Lindqvist clusters $\{[Cu(NH_3)_4(H_2O)]_2[Nb_2W_4O_{19}]\cdot 8H_2O$ (**2**)}, and four phases of the Lindqvist clusters are linked in a two-dimensional array by (amine)copper complexes $\{[Cu(dap)_2]_3[Nb_4W_2O_{19}]\cdot 7H_2O$ (**3**), $[Cu(dap)_2]_3[H_2Nb_6O_{19}]\cdot 6H_2O$ (**4**), $[Cu(dap)_2]_3[Nb_3W_3O_{19}]\cdot Cl\cdot 6H_2O$ (**5**), and $[Cu(en)_2]_3[Nb_4W_2O_{19}]\cdot 6H_2O$ (**6**)}.

Results and Discussion

Syntheses and Diffuse Reflectance Spectroscopy

Table 1 summarizes the reaction conditions used to obtain compounds **1**–**6** and compares them to the methods we previously reported for one-dimensional chain materials, a dimer, and a supramolecular complex containing $[H_9Nb_{24}O_{72}]^{15-}$ (Reactions A–E).[18,36] In the previous stud-

Table 1. Summary of synthesis conditions for (amine)copper isopolyniobate phases.

Reaction	Cluster source[a] (conc., mmol)	Ligand[b] (H_2O/amine)	Cu equiv. per cluster	Product	Structure (Cu coordination mode)
A	$RbNb_6$ (22)	en (15:1)	4	$Rb_4[Cu(en)_2(H_2O)_2]_3[(H_2Nb_6O_{19})_2Cu(en)_2]$	dimer (linked, charge-balanced)
B	$RbNb_6$ (11)	en (15:1)	8	$[Cu(en)_2(H_2O)_2]_2[(H_2Nb_6O_{19})Cu(en)_2]$	1-dimensional (linked, charge-balanced)
C	$RbNb_6$ (33)	NH_3 (30:1)	3	$Rb_2[Cu(NH_3)_2(H_2O)_4][Cu(NH_3)_4(H_2O)_2]_2\text{-}\{[Nb_6O_{19}][Cu(NH_3)]_2\}_2$	1-dimensional (linked, charge-balanced)
D	$RbNb_6$ (7.5)	NH_3 (11:1)	3	$\{[Nb_6O_{19}][Cu(NH_3)_2(H_2O)]_2[Cu(H_2O)_4]_2\}$	1-dimensional[c] (linked)
E	$RbNb_6$ (24)	en (3:1)	4	$(H_2en)_6[Cu(en)_2(H_2O)_2]_3[(\{H_9Nb_{24}O_{72}\}\{Cu(en)_2\text{-}(H_2O)\}_2\{Cu(en)_2\})_2]$	Nb_{24}[d] (linked, charge-balanced, decorated)
F	KNb_6 (11)	en (15:1)	4	$[Cu(en)_2(H_2O)_2]_2[(H_2Nb_6O_{19})Cu(en)_2]$	1-dimensional (linked, charge-balanced)
G	Nb_{10} (13)	en (7:1)	4	$(H_2en)_6[Cu(en)_2(H_2O)_2]_3[(\{H_9Nb_{24}O_{72}\}\{Cu(en)_2\text{-}(H_2O)\}_2\{Cu(en)_2\})_2]$	Nb_{24}[d] (linked, charge-balanced, decorated)
H	Nb_2W_4 (41)	en (H_2O)[e]	2	$[Cu(en)_2(H_2O)]_2[Nb_2W_4O_{19}]\cdot 2H_2O$ (**1**)	monomer (decorated)
I	Nb_2W_4 (41)	NH_3 (H_2O)[e]	2	$[Cu(NH_3)_4(H_2O)]_2[Nb_2W_4O_{19}]\cdot 8H_2O$ (**2**)	monomer (charge-balanced)
J	Nb_4W_2 (23)	dap (34:1)	3	$[Cu(dap)_2]_3[Nb_4W_2O_{19}]\cdot 7H_2O$ (**3**)	2-dimensional (linked)
K	Nb_{10} (6)	dap (12:1)	4	$[Cu(dap)_2]_3[H_2Nb_6O_{19}]\cdot 6H_2O$ (**4**)	2-dimensional (linked)
L	Nb_2W_4 (25)	dap (30:1)	2	$[Cu(dap)_2]_3[Nb_3W_3O_{19}]\cdot Cl\cdot 6H_2O$ (**5**)	2-dimensional (linked)
M	Nb_4W_2 (26)	en (23:1)	3	$[Cu(en)_2]_3[Nb_4W_2O_{19}]\cdot 6H_2O$ (**6**)	2-dimensional (linked)

[a] $RbNb_6 = Rb_8[Nb_6O_{19}]$; $KNb_6 = K_8[Nb_6O_{19}]$; $Nb_2W_4 = [N(CH_3)_4]_2Na_2[cis\text{-}Nb_2W_4O_{19}]$; $Nb_4W_2 = Na_4K_2[Nb_4W_2O_{19}]$; $Nb_{10} = [N(CH_3)_4]_6[Nb_{10}O_{28}]$. [b] en = ethylenediamine; dap = 1,3-diaminopropane. [c] Reaction gives two phases of neutral chains with no counterions. [d] $Nb_{24} = [H_9Nb_{24}O_{72}]^{15-}$. [e] Amine is ligand only, negligible amount in the solvent.

ies, $Rb_8[Nb_6O_{19}]\cdot 14H_2O$ was the sole source of the Lindqvist ion. However, crystallographic and SAXS studies indicate that there is a strong association between Rb^+ and $[Nb_6O_{19}]^{8-}$ in both the solid state and solution.[16,40] This prompted us to investigate systems with other cations {Na^+, K^+, and $[N(CH_3)_4]^+$} that do not strongly associate with the polyanion. For example, when $K_8[Nb_6O_{19}]$ is used instead of $Rb_8[Nb_6O_{19}]$ in Reaction B, the same product could be obtained by using 50% less $Cu(NO_3)\cdot 2.5H_2O$ (i.e. using a stoichiometric amount of Cu^{II} instead of 100% excess) (Reaction F). Likewise, $[N(CH_3)_4]_6[Nb_{10}O_{28}]$ can be used instead of $Rb_8[Nb_6O_{19}]$ to obtain higher yields of $(H_2en)_6[Cu(en)_2(H_2O)_2]_3[(\{H_9Nb_{24}O_{72}\}\{Cu(en)_2(H_2O)\}_2\{Cu(en)_2\})_2]$ (Reaction G).

In the present study, cluster sources were utilized with charge densities ranging from 0.16 to 0.32 charge/atom (Reactions F–M). The term “cluster source” is used because $[Nb_{10}O_{28}]^{6-}$ is not a Lindqvist ion but rapidly forms $[H_nNb_6O_{19}]^{(8-n)-}$ ($n = 0 - 3$) in basic solution.[39] This provides an alkali-metal-free source of $[H_nNb_6O_{19}]^{(8-n)-}$, because its counterions are $[N(CH_3)_4]^+$. The cluster studied here with the lowest charge and lowest charge density, $[cis\text{-}Nb_2W_4O_{19}]^{4-}$, required mild reaction conditions (60 °C, pH = 9.5) in basic solution (with NH_4OH or en) in order to prevent decomposition of the cluster. However, in the presence of dap, $[cis\text{-}Nb_2W_4O_{19}]^{4-}$ was converted into $[fac\text{-}Nb_3W_3O_{19}]^{5-}$ at ambient temperature. The clusters of intermediate charge density ($[H_2Nb_6O_{19}]^{6-}$ and $[cis\text{-}Nb_4W_2O_{19}]^{6-}$) proved to be the most versatile, because they had the highest solubility and the widest pH stability range.

Prolonged heating at 95 °C in a mixed water/amine (en or dap) solution was necessary for the synthesis of **3**, **4**, **5**, and **6** (Reactions J–M). Under these conditions, the ratio of H_2O/en or dap in the solvent becomes lower, because the boiling points of en and dap (118 °C and 140 °C, respectively) are somewhat higher than that of H_2O. As a result, very small crystals of **3**, **4**, **5**, and **6** form rapidly upon cooling of the solution to ambient temperature, because they are much less soluble in the amine than they are in water. Larger crystals of **3** and **5** were obtained by slightly increasing the H_2O/dap ratio by the addition of aqueous 6 M HCl to form the $[NH_3CH_2CH_2CH_2NH_3]Cl_2$ salt.

The visible diffuse reflectance spectra for complexes **1**–**6** are illustrated in Figure 1. All six of the complexes display a broad band centered from 395 nm to 425 nm. Previous studies have established that this band may be attributed to the d–d transitions of the Cu^{II} centers[41–43] and is verified by comparison with authentic samples of $Cu(en)_2(NO_3)_2$ and $Cu(dap)_2(NO_3)_2$. Complexes **1** and **6** feature a $Cu(en)_2$ complex and display a redshift of 41 and 29 nm, respectively, relative to $Cu(en)_2(NO_3)_2$. Similar observations are made for complexes **3**, **4**, and **5**, which feature a $Cu(dap)_2$ complex and display redshifts of 24, 28, and 24 nm, respectively, relative to $Cu(dap)_2(NO_3)_2$. Differences in the reflectance intensity may be attributed to the mass percent of Cu^{II} present in the compounds when the Cu^{II} centers are in very similar ligand environments and at relatively low concentrations.[43] For example, complexes **3** and **5** both display $\lambda_{max} = 397$ nm, but complex **3** has weaker reflectance than **5** due to the fact that the mass percentage of Cu^{II} present in **3** (10.6%) is higher than in **5** (10.0%).

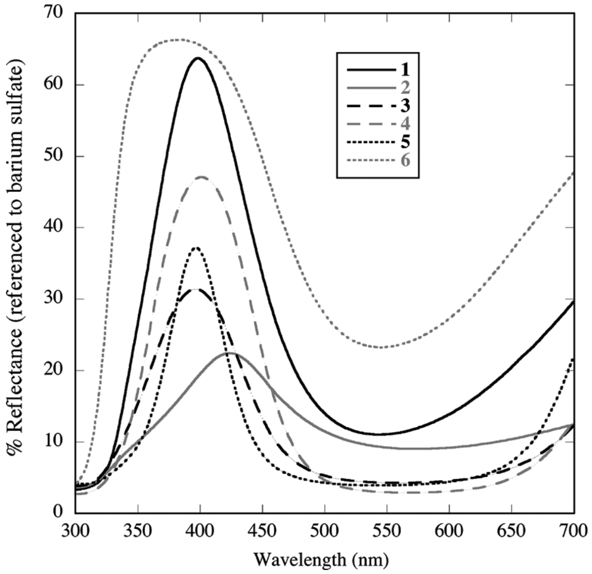

Figure 1. Visible diffuse reflectance spectra for complexes **1**–**6** referenced to barium sulfate (100% reflectance).

Description of the Structures

In the structures of **1**, **2**, **3**, and **6**, the composition and isomer of the Lindqvist ion reflects that of the precursor Lindqvist salt. For **4** and **5**, $[Nb_{10}O_{28}]^{6-}$ and $[cis\text{-}Nb_2W_4O_{19}]^{4-}$ have converted into $[H_2Nb_6O_{19}]^{6-}$ and $[fac\text{-}Nb_3W_3O_{19}]^{5-}$, respectively, in the alkaline reaction media. For each mixed addenda structure, with the exception of **1**, the clusters are completely disordered in their orientation in the crystal lattice. From a structural perspective, this means that the occupancy of each metal site within the cluster represents the W/Nb ratio of the entire cluster. This was confirmed crystallographically by initially allowing the W/Nb ratio of each site to refine freely, followed by fixing it to give a whole number ratio of metals in the cluster (i.e. W/Nb = 0.67:0.33 for **1** and **2**, W/Nb = 0.33:0.67 for **3** and **6**, and W/Nb = 0.5:0.5 for **5**). The major bond lengths for all six structures are averaged and summarized in Table 2. These include the metal–oxygen bond lengths of the Lindqvist cluster, the $Cu–O_{water}$ and $Cu–O_{cluster}$ bond lengths, and the $Cu–N_{amine}$ bond lengths. In general, the Nb–O bonds are longer than the W–O bonds. Similarly, in mixed Nb/W sites, higher Nb/W ratio sites have longer M–O bonds. The Cu–N bond lengths are ~2 Å for all the amines (NH_3, en, and dap) and the $Cu–O_{cluster}$ and $Cu–O_{water}$ bond lengths range from 2.5 to 2.9 Å.

The reaction of $[N(CH_3)_4]_2Na_2[cis\text{-}Nb_2W_4O_{19}]$ with a $Cu(NH_3)$ complex in aqueous solution (Table 1, Reaction I) resulted in a phase featuring isolated clusters (**2**). A view of

Table 2. Selected average bond lengths [Å] for structures **1**–**6**.[a]

Structure	M=O_t	M–O_c	M–O_b	Cu–N	Cu–O
$[Cu(en)_2(H_2O)]_2[Nb_2W_4O_{19}]\cdot 2H_2O$ (**1**)				2.017	2.553
$W_{1.0}$ (W1)	1.721	2.326	1.929		
$W_{0.5}Nb_{0.5}$ (W/Nb2, W/Nb3)	1.742	2.343	1.956		
$[Cu(NH_3)_4(H_2O)]_2[Nb_2W_4O_{19}]\cdot 8H_2O$ (**2**)				2.006	2.897
$W_{0.67}Nb_{0.33}$ (W/Nb1)	1.762	2.347	1.953		
$[Cu(dap)_2]_3[Nb_4W_2O_{19}]\cdot 7H_2O$ (**3**)				2.021	2.878
$W_{0.33}Nb_{0.67}$ (W/Nb1)	1.761	2.348	1.966		
$[Cu(dap)_2]_3[H_2Nb_6O_{19}]\cdot 6H_2O$ (**4**)				2.026	2.833
$Nb_{1.0}$ (Nb1)	1.775	2.383	2.006		
$[Cu(dap)_2]_3[Nb_3W_3O_{19}]\cdot Cl\cdot 6H_2O$ (**5**)				2.011	2.921
$W_{0.5}Nb_{0.5}$ (W/Nb1)	1.756	2.342	1.964		
$[Cu(en)_2]_3[Nb_4W_2O_{19}]\cdot 6H_2O$ (**6**)				2.006	2.739
$W_{0.33}Nb_{0.67}$ (W/Nb1)	1.773	2.345	1.964		

[a] M = W/Nb, as indicated; O_t = terminal oxygen atom; O_c = central μ_6-oxygen atom; O_b = bridging μ_2-oxygen atom.

2 is shown in Figure 2, and it illustrates that the clusters are in a distorted hexagonal packing arrangement within the (001) plane. The cluster layers stack in a manner similar to cubic close-packed objects along the *c*-axis. Also aligned parallel to the *c*-axis are chains of alternating $[Cu(NH_3)_4]^{2+}$ ions and water molecules. The Cu^{II} ion sits in a square plane of nitrogen atoms, with a Cu–N distance of 2.015(7) Å, and it is 2.871(8) Å away from the water oxygen atoms that sit in the axial position of the copper octahedron, $[Cu(NH_3)_4(H_2O)_2]^{2+}$. The water molecules (O8) between the Cu^{II} ions in chains are located on two half-occupied positions, 0.77 Å apart. However, to optimize the displacement parameters of this water site, we fixed it on a special position that is one-fourth occupied, between the two one-half occupied sites. This gives the appearance of straight Cu–O–Cu chains (with a 180° angle) in Figure 2. However, in reality, the angle is less than 180°, and the water molecule resonates around its crystallographically fixed position. There are two additional water sites providing eight water molecules per cluster that sit between the clusters and are within H-bonding distance from each other, from the terminal cluster oxygen atoms, and from the Cu-linked water molecule (O···O ~2.6–2.8 Å).

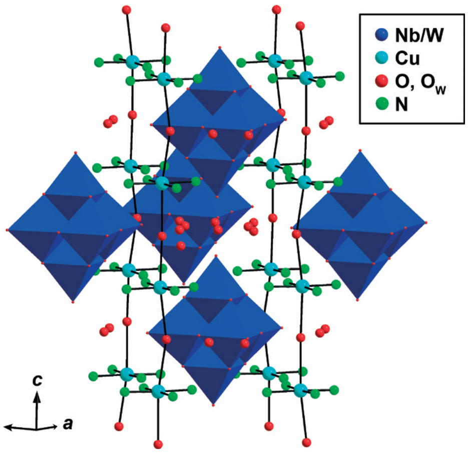

Figure 2. View of **2** in combination polyhedral/ball-and-stick notation.

The reaction of $[N(CH_3)_4]_2Na_2[cis\text{-}Nb_2W_4O_{19}]$ with a Cu(en) complex in aqueous solution (Table 1, Reaction H) resulted in a phase with clusters decorated by copper complexes (**1**). This is the only structure with partial ordering of the mixed addenda Lindqvist cluster orientation in the lattice. Although ^{183}W MAS NMR spectroscopy of **1** could not be executed to confirm the *cis* isomer (due to the paramagnetic Cu^{II} centers), the terminal and bridging M=O_t and M–O_b–M (M = W, Nb) vibrations observed in the infrared spectrum of **1** are similar to that of the precursor salt[32] [although partially masked by vibrations of the Cu(en) complex], suggesting that **1** contains primarily the $[cis\text{-}Nb_2W_4O_{19}]^{4-}$ isomer. The cluster has three crystallographically unique sites with a multiplicity of two within the cluster, and the replicate sites are arranged in a *trans* fashion. Refinement of the cluster metal site occupancies was optimized with one site being fully occupied by W and the other two sites with one-half Nb and one-half W. This gives a square plane of Nb/W sites and W-only sites in the axial position of the superoctahedron (Figure 3). Therefore, the Cu^{II} ion is always bonded to Nb–O_b–Nb or W–O_b–Nb oxygen atoms. A similar observation was made by Klemperer and Day in a structure of $[cis\text{-}Nb_2W_4O_{19}]^{4-}$ complexed to Rh.[44] In **1**, each $[cis\text{-}Nb_2W_4O_{19}]^{4-}$ has two $[Cu(en)_2\text{-}H_2O]^{2+}$ complexes bonded on opposite edges. The Cu–$O_{cluster}$ bond length is 2.740(5) Å and the Cu–O_{water} bond length is 2.366(6) Å. The copper–oxygen bond lengths found here are similar to those observed in other cupric $[Nb_6O_{19}]^{8-}$ structures.[18,19,36] The $[cis\text{-}Nb_2W_4O_{19}]^{4-}$ and $[Cu(en)_2(H_2O)]^{2+}$ complexes are arranged in the crystal lattice with each Cu–cluster–Cu axis perpendicular to that of the neighboring complex [approximately parallel to (011) or (0–11)].

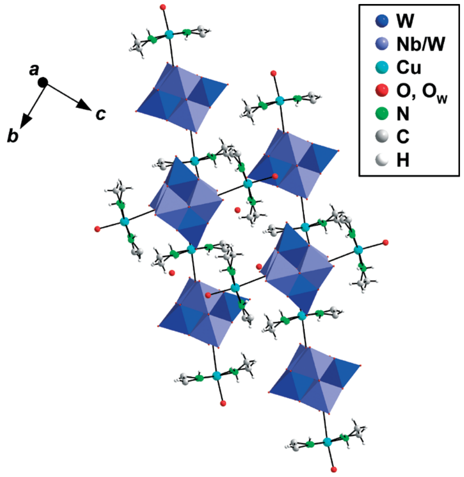

Figure 3. View of **1** in combination polyhedral/ball-and-stick notation.

The structures of **3**, **4**, **5**, and **6** are all very similar. The framework of these structures consists of a Lindqvist ion that is linked to six CuL_2 (L = dap or en) moieties. Three CuL_2 complexes are bonded to adjacent M–O_b–M (M = W, Nb) bridging oxygen atoms on two opposite faces of the super-octahedral cluster (see Figure 4), and thus the copper-bound face has a perpendicular $\bar{6}$ rotation axis that is parallel to the *c*-axis of the unit cell. Each copper atom bridges two clusters with a Cu–O_b bond length around 2.8 Å for all four structures. Since the copper atoms are bonded to opposite faces of the Lindqvist cluster, this gives an overall framework that can be described as layered or two-dimensional with alternate layers of copper complexes and clusters. These are illustrated in two views in Figure 5. The phase in which Cu^{II} is coordinated to en (**6**) crystallizes in the $R\bar{3}m$ space group, and the three phases (**3**, **4**, and **5**) in which Cu^{II} coordinates to dap crystallize in the $R\bar{3}c$ space group, with the *c*-axis approximately doubled to that of **6** via a glide in the (110) plane. This is best viewed along the *c*-axis (Figure 6). The phases **3**, **4**, and **6** were obtained from two cluster compositions with a 6– charge, $[H_2Nb_6O_{19}]^{6-}$ and $[cis\text{-}Nb_4W_2O_{19}]^{6-}$, and the clusters are charge-balanced by three Cu^{II} complexes.

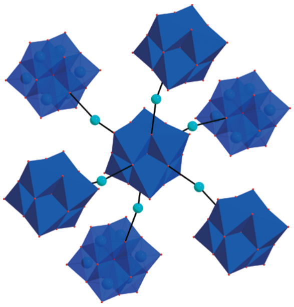

Figure 4. View of the Cu hexametalate cluster linkage geometry featured in structures **3**, **4**, **5**, and **6** along a $\bar{6}$ rotation axis. The clusters represented by solid octahedra are linked through copper atoms (turquoise spheres) to the up-face of the central cluster, and the clusters with transparent octahedra are linked through copper atoms to the down-face of the central cluster.

The structure of **5** was initially solved by using the atomic positions of **4** and a cluster composition of $[cis\text{-}Nb_2W_4O_{19}]^{4-}$. However, a large peak remained in the electron density map. Energy dispersive spectroscopy (EDS) indicated this unidentified atom was chlorine. This agreed well with the displacement parameters, but it did not solve the problem of charge-balance. Upon changing the occupancy of the W/Nb sites to 50%/50% instead of the initially expected 67%/33%, the *R* value went down ~1%, and a free refinement of the occupancy gave a value of 49.46% W. Therefore, a cluster composition of $[fac\text{-}Nb_3W_3O_{19}]^{5-}$ plus a Cl^- ion charge-balance the three copper complexes. This assignment is also supported by elemental analyses and by

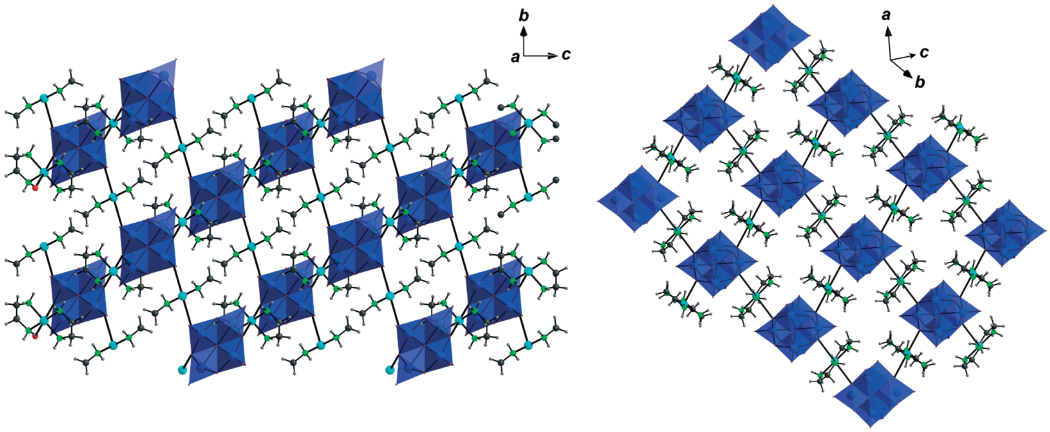

Figure 5. Two different views of the two-dimensional linkage of Lindqvist ions and (amine)copper complexes featured in structures **3**, **4**, **5**, and **6**. The blue polyhedra are the Nb/WO_6 octahedra of the Lindqvist clusters, and the turquoise spheres are the Cu^{II} cations ligated by diamines.

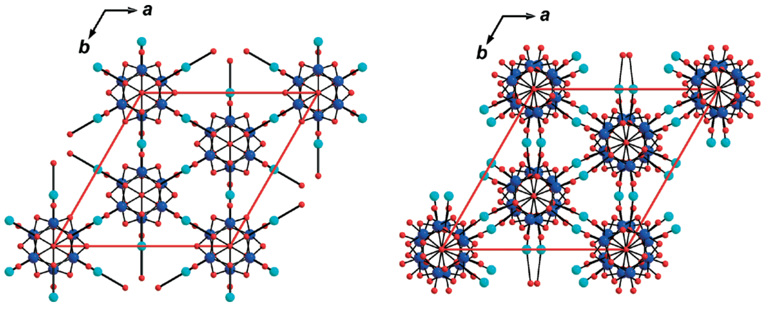

Figure 6. Views along the *c*-axis showing the difference between the symmetry of compound **6** (left; $R\bar{3}m$ space group) and **3**, **4**, and **5** (right; $R\bar{3}c$ space group). The $R\bar{3}m$ space group is obtained when en is ligated to Cu, and the $R\bar{3}c$ space group is obtained when dap is ligated to Cu. The amine ligands are omitted for ease of viewing. The turquoise spheres are Cu, the blue spheres are Nb/W, and the red spheres are O.

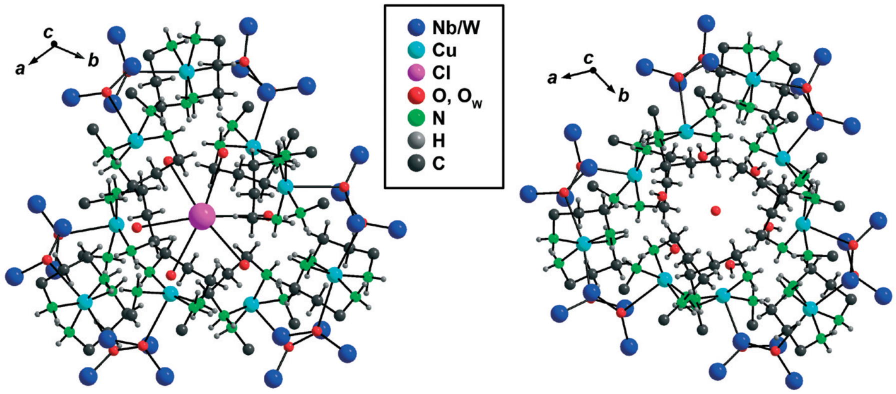

Figure 7. View of the extra-framework site of structures **3**, **4**, **5**, and **6** that contains a chlorine ion in structure **5** (left), a water molecule in structure **3** (right), and is vacant in structures **4** and **6**.

the infrared spectrum of **5**, which has a doublet of peaks between 500 and 550 cm^{-1}, that is very similar to that of $[N(CH_3)_4]Na_2K_2[$*fac*$\text{-}Nb_3W_3O_{19}]\cdot H_2O$.[31,32] The Cl^- ion is surrounded by six water molecules in a distorted octahedral arrangement with a $Cl\cdots O_{water}$ distance of 3.275 Å, which is similar to that observed in hydrate chloride salts of aluminum and cobalt. The chlorine ions sit in a channel, as observed in Figure 7, and it is most likely obtained from the HCl added in the synthesis in order to partially neutralize dap to obtain larger crystals.

The structure of **3** has a position similar to the Cl^- site in **5**, but it is occupied by a water molecule with the surrounding six water molecules at a distance of ~2.8 Å (also shown in Figure 7). This site appears to be vacant in the crystal lattices of **4** and **6**, so these may be considered partially dehydrated versions of this structural motif of Lindqvist ions alternately layered with (diamine)copper complexes. The Lindqvist clusters of **3**, **5**, and **6** have mixed W/Nb metal sites that are completely disordered in the crystal lattice. In addition, the protons of the $[H_2Nb_6O_{19}]^{6-}$ cluster of **4** were not located in the electron density map, but they are required for charge-balancing. Diprotonation of $[Nb_6O_{19}]^{8-}$ has been observed in both alkali salts and (amine)copper complexes,[12,16,18] and therefore it is a reasonable assumption for charge-balancing the framework of **4**. These protons most likely reside on the cluster faces that are not bonded to Cu.

Conclusions

The high charge density of $[Nb_6O_{19}]^{8-}$ and its stability and solubility in almost exclusively basic, aqueous media have limited the use of this cluster in the formation of d- and f-electron-containing materials. In this paper we have investigated the use of lower charge density Lindqvist clusters in mixed-solvent/complex systems as a means of circumventing the preceding problems. The reactions studied in Table 1 may be classified into one of three groups according to the charge density of the Lindqvist cluster or cluster source used. The difference is not trivial, the charge density of [*cis*-$Nb_2W_4O_{19}]^{4-}$ (group one, lowest charge density) is 50% lower than that of [*cis*-$Nb_4W_2O_{19}]^{6-}$ (group two, intermediate charge density) and 100% lower than that of $[Nb_6O_{19}]^{8-}$ (group three, highest charge density).

The cluster with the lowest charge and charge density, [*cis*-$Nb_2W_4O_{19}]^{4-}$, reacts with $Cu(NH_3)$ in water to form a compound that is charge-balanced by the d-electron metal complex, but it reacts with Cu(en) under almost identical conditions (including pH) to form a compound that is decorated by the d-electron metal complex. Likewise, $[Nb_{10}O_{28}]^{6-}$ reacts with Cu(en) to form a compound containing $[H_9Nb_{24}O_{72}]^{15-}$ that is linked, decorated, and charge-balanced by the d-electron metal complex, but under similar conditions (assuming that the difference in the basicity of en and dap in the mixed-solvent/complex system is small), $[Nb_{10}O_{28}]^{6-}$ reacts with Cu(dap) to form a phase containing $[H_2Nb_6O_{19}]^{6-}$ Lindqvist ions that are linked to $Cu(dap)_2$ in a two-dimensional array. The results suggest that the low-charge-density clusters may be templated by coordination complexes to form new phases.

The Lindqvist ions of intermediate charge density (i.e. charge density higher than that of [*cis*-$Nb_2W_4O_{19}]^{4-}$ but lower than that of $[Nb_6O_{19}]^{8-}$), including [*fac*-$Nb_3W_3O_{19}]^{5-}$, [*cis*-$Nb_4W_2O_{19}]^{6-}$, and alkali-metal-free $[H_2Nb_6O_{19}]^{6-}$, all form virtually isostructural two-dimensional arrays linked by CuL_2 (L = en or dap) regardless of the cluster composition or coordinating amine. In contrast to $[H_2Nb_6O_{19}]^{6-}$, isoelectronic [*cis*-$Nb_4W_2O_{19}]^{6-}$ forms a two-dimensional structure in the presence of alkali cations. This is most likely due to the lower symmetry of [*cis*-$Nb_4W_2O_{19}]^{6-}$ and the asymmetric distribution of charge on its surface.

A two-dimensional material could not be prepared from $[Nb_6O_{19}]^{8-}$ (K^+ or Rb^+ salt) under the reaction conditions studied here, but in previous studies $Rb_8[Nb_6O_{19}]$ did form one-dimensional linked assemblies with two to four Cu-cluster bonds per Lindqvist ion. All of the structures reported here that were synthesized from $[N(CH_3)_4]^+$, Na^+, and K^+ cluster salts yield products that are alkali-metal-free. In contrast, the analogous syntheses from $Rb_8[Nb_6O_{19}]$ usually resulted in phases containing Rb^+ except when a large excess of Cu^{II} was added. The work presented here builds on the evidence that $[Nb_6O_{19}]^{8-}$ undergoes unusually strong and extensive associations with counter-cations in solution. In fact, there are increasing indications that ion pairing strongly affects and directs the behavior of polyoxoniobates in solution, and understanding, controlling, or exploiting it may be a key factor to enhance the strategic development of this chemistry.

Experimental Section

General Methods and Materials: $[N(CH_3)_4]_6[Nb_{10}O_{28}]\cdot 6H_2O$,[38,39] $[N(CH_3)_4]_2Na_2[cis\text{-}Nb_2W_4O_{19}]\cdot 18H_2O$,[31] and $Na_4K_2[cis\text{-}Nb_4W_2O_{19}]\cdot 12H_2O$[31] were obtained as previously reported and their purity was confirmed by IR and ^{17}O or ^{183}W NMR spectroscopy. $Cu(NO_3)_2\cdot 2.5H_2O$ (Certified A.C.S.), HCl (Certified A.C.S. Plus), and NH_4OH (Certified A.C.S. Plus) were purchased from Fisher. Ethylenediamine (en, $NH_2CH_2CH_2NH_2$; ReagentPlus ≥ 99%) and 1,3-diaminopropane [dap, $NH_2(CH_2)_3NH_2$; 99%] were purchased from Aldrich. Compositional analyses (Cl, Cu, Nb, and W) were performed by SEM-EDS and/or Galbraith Laboratories, Inc. IR spectra were recorded with a Thermo Nicolet 380 FT-IR instrument equipped with a Smart Orbit (Diamond) ATR accessory. For visible diffuse reflectance spectrometry (Vis-DRS), a Shimadzu UV-3600 UV/Vis/NIR instrument was used. The system operates with an integrating sphere 150 mm in inner diameter and is equipped with a photomultiplier and a PbS cell. The spectral range was 300–700 nm with a spectral resolution of 1 nm and a slit width of 20 nm. All reflectance values are referenced to $BaSO_4$ (100% reflectance).

Synthesis of $Cu(en)_2(NO_3)_2$ and $Cu(dap)_2(NO_3)_2$: $Cu(en)_2(NO_3)_2$ and $Cu(dap)_2(NO_3)_2$ were synthesized as reference compounds for the Vis-DRS studies. A 0.5 g sample of $Cu(NO_3)_2\cdot 2.5H_2O$ was dissolved in 10 g of CH_3OH, and either en or dap was added until a shiny, purple plate-like precipitate formed. The solids were collected by vacuum filtration. The sample of $Cu(en)_2(NO_3)_2$ was identified by matching its X-ray powder pattern with the reported structures,[45,46] and single-crystal X-ray diffraction data was collected on $Cu(dap)_2(NO_3)_2$ after it was recrystallized from methanol at –10 °C. Both structures feature Cu^{II} in octahedral coordination bonded to four nitrogen atoms in a square plane (~2 Å) and two *trans* oxygen atoms of the nitrate anions (~2.5 Å), and they are ideal standards for the similarly ligated Cu^{II} complexes of structures **1**–**6**.

Synthesis of $[Cu(en)_2(H_2O)]_2[Nb_2W_4O_{19}]\cdot 2H_2O$ (1): A 1 g sample of $[N(CH_3)_4]_2Na_2[cis\text{-}Nb_2W_4O_{19}]\cdot 18H_2O$ (0.53 mmol) was dissolved in 10 mL of H_2O with stirring and heating to 60 °C, and 0.27 g of $Cu(NO_3)_2\cdot 2.5H_2O$ (1.2 mmol) dissolved in 3 mL of H_2O was added dropwise. The pH of the solution was increased to ~9.5 by slow addition of en. The slightly cloudy solution was syringe-filtered (0.45 µm) warm and allowed to slowly concentrate in air. After 1–3 d, 0.35 g (40% yield) of purple columnar crystals was collected by suction filtration, washed with methanol, and dried in vacuo. IR (ATR, 1100–400 cm^{-1}): $\tilde{\nu}_{max}$ = 1035 (m), 950 (sh), 930 (m), 882 (m), 758 (s), 708 (s), 561 (s) cm^{-1}. $C_8H_{40}Cu_2N_8Nb_2O_{23}W_4$ (1664.7): calcd. Cu 7.6, Nb 11.2, W 44.2; found Cu 7.3, Nb 11.8, W 44.1.

Synthesis of $[Cu(NH_3)_4(H_2O)]_2[Nb_2W_4O_{19}]\cdot 8H_2O$ (2): A 1 g sample of $[N(CH_3)_4]_2Na_2[cis\text{-}Nb_2W_4O_{19}]\cdot 18H_2O$ (0.53 mmol) was dissolved in 10 mL of H_2O with stirring and heating to 60 °C. The solution was cooled to room temperature, and 0.27 g of $Cu(NO_3)_2\cdot 2.5H_2O$ (1.2 mmol) dissolved in 3 mL of H_2O was added dropwise. The pH of the solution was increased to ~9.5 by slow addition of concentrated NH_4OH. The solution was syringe-filtered (0.45 µm) and allowed to concentrate in air. After 1–3 d, well-formed, octahedron-shaped crystals grew. The product (0.15 g, 17% yield) was collected by suction filtration, washed with methanol, and dried in vacuo. IR (ATR, 1100–400 cm^{-1}): $\tilde{\nu}_{max}$ = 925 (sh), 863 (m), 713 (s), 552 (s) cm^{-1}. $H_{44}Cu_2N_8Nb_2O_{29}W_4$ (1668.6): calcd. Cu 7.6, Nb 11.1, W 44.1; found Cu 7.4, Nb 10.9, W 44.3.

Synthesis of $[Cu(dap)_2]_3[Nb_4W_2O_{19}]\cdot 7H_2O$ (3): A 0.15 g sample of $Cu(NO_3)_2\cdot 2.5H_2O$ (0.64 mmol) was dissolved in 2 mL of H_2O, and 1 g (13 mmol) of dap was added to 1 mL of H_2O in a separate 20 mL glass scintillation vial. The $Cu(NO_3)_2$ solution was added to the dap/H_2O mixture, and the resulting compound was added dropwise to a 0.30 g sample of $Na_4K_2[Nb_4W_2O_{19}]\cdot 12H_2O$ (0.21 mmol) dissolved in 5 mL of H_2O by heating to ~60 °C and stirring. The solution was then heated to ~95 °C and stirred until the volume was reduced by 10–15%. Upon cooling to ~60 °C, a 1-mL aliquot of 6 M HCl was added dropwise with vigorous stirring. The solution was syringe-filtered (0.45 µm) warm and allowed to slowly concentrate in air. After 3–4 d, 0.014 g (4% yield) of purple crystals with a block-like morphology was collected by suction filtration, washed with ethanol, and dried in vacuo. IR (ATR, 1100–400 cm^{-1}): $\tilde{\nu}_{max}$ = 1048 (m), 906 (m), 874 (sh), 849 (s), ~700 (s), 534 (m), 499 (m) cm^{-1}. $C_{18}H_{74}Cu_3N_{12}Nb_4O_{26}W_2$ (1804.8): calcd. Cu 10.6, Nb 20.6, W 20.4; found Cu 10.1, Nb 20.9, W 20.8.

Synthesis of $[Cu(dap)_2]_3[H_2Nb_6O_{19}]\cdot 6H_2O$ (4): A 0.068 g sample of $Cu(NO_3)_2\cdot 2.5H_2O$ (0.29 mmol) was dissolved in 1 mL of H_2O, and 3 g (40 mmol) of dap was added to 4 mL of H_2O in a separate 20 mL glass scintillation vial. The $Cu(NO_3)_2$ solution was added to the dap/H_2O mixture, and the resulting solution was added dropwise to a 0.14 g sample of $[N(CH_3)_4]_6[Nb_{10}O_{28}]\cdot 6H_2O$ (0.073 mmol) dissolved in 4 mL of H_2O. The solution was heated (~95 °C) and stirred until the volume was reduced by 25–40%. The solution was syringe-filtered (0.45 µm) warm and allowed to slowly concentrate in air. After 2–5 d, 0.06 g (57% yield) of purple microcrystalline powder was collected by suction filtration, washed with ethanol, and dried in vacuo. IR (ATR, 1100–400 cm^{-1}): $\tilde{\nu}_{max}$ = 1048 (m), 908 (m), 848 (s), 733 (sh), ~660 (s), 559 (sh), 530 (s), 495 (s), 415 (s) cm^{-1}. $C_{18}H_{74}Cu_3N_{12}Nb_6O_{25}$ (1606.9): calcd. Cu 11.9, Nb 34.7; found Cu 12.0, Nb 36.3.

Synthesis of $[Cu(dap)_2]_3[Nb_3W_3O_{19}]\cdot Cl\cdot 6H_2O$ (5): A 0.10 g sample of $Cu(NO_3)_2\cdot 2.5H_2O$ (0.43 mmol) was dissolved in 1 mL of H_2O, and 1 g (13 mmol) of dap was added to 1 mL of H_2O in a separate 20 mL glass scintillation vial. The $Cu(NO_3)_2$ solution was added to the dap/H_2O mixture, and the resulting compound was added dropwise to a 0.375 g sample of $[N(CH_3)_4]_2Na_2[cis\text{-}Nb_2W_4O_{19}]\cdot 18H_2O$ (0.20 mmol) dissolved in 5 mL of H_2O by heating to ~60 °C and stirring. The temperature was increased to ~95 °C, and the solution was continually stirred until the volume was reduced by 10–15%. Upon cooling to ~60 °C, a 1-mL aliquot of 6 M HCl was added dropwise with vigorous stirring. The solution was syringe-filtered (0.45 µm) warm and allowed to slowly concentrate in air. After 1 d, 0.047 g (17% yield based on Nb) of purple block-shaped crystals was collected by suction filtration, washed with ethanol, and dried in vacuo. IR (ATR, 1100–400 cm^{-1}): $\tilde{\nu}_{max}$ = 1044 (m), ~920 (sh), 871 (m), 750 (s), 704 (s), 554 (s), 501 (s) cm^{-1}. $C_{18}H_{74}ClCu_3N_{12}Nb_3O_{25}W_3$ (1915.2): calcd. Cl 1.9, Cu 10.0, Nb 14.6, W 28.8; found Cl 1.5, Cu 10.3, Nb 15.6, W 28.5.

Synthesis of $[Cu(en)_2]_3[Nb_4W_2O_{19}]\cdot 6H_2O$ (6): A 0.30 g sample of $Cu(NO_3)_2\cdot 2.5H_2O$ (1.3 mmol) was dissolved in 2 mL of H_2O, and 2 g of en (33 mmol) was added to 2 mL of H_2O in a separate 20 mL glass scintillation vial. The $Cu(NO_3)_2$ solution was added to the en/H_2O mixture, and the resulting solution was added dropwise to a

Table 3. Crystallographic information for structures **1**–**6**.

Compound	**1**	**2**	**3**	**4**	**5**	**6**
Empirical formula	$C_8H_{40}N_8O_{23}$-$Cu_2Nb_2W_4$	$H_{44}N_8O_{29}$-$Cu_2Nb_2W_4$	$C_{18}H_{74}N_{12}O_{26}$-$Cu_3Nb_4W_2$	$C_{18}H_{74}N_{12}O_{25}$-Cu_3Nb_6	$C_{18}H_{74}ClN_{12}O_{25}$-$Cu_3Nb_3W_3$	$C_{12}H_{60}N_{12}O_{25}$-$Cu_3Nb_4W_2$
Formula mass	1664.7	1668.6	1804.8	1606.9	1915.2	1702.6
Crystal system	monoclinic	tetragonal	trigonal	trigonal	trigonal	trigonal
Space group	$P121/n1$ (no. 14)	$I4/m$ (no. 87)	$R\bar{3}c$ (no. 167)	$R\bar{3}c$ (no. 167)	$R\bar{3}c$ (no. 167)	$R\bar{3}m$ (no. 166)
a [Å]	10.390(1)	11.292(1)	14.838(3)	14.788(1)	15.0169(7)	14.580(6)
b [Å]	14.494(2)					
c [Å]	10.813(1)	11.485(1)	37.011(8)	37.313(5)	36.7009(36)	17.7355(103)
β [°]	96.487(2)					
V [Å^3]	1618.0(5)	1464.4(2)	7057(3)	7067(1)	7167.50(85)	3265.04(268)
Z	2	2	6	6	6	3
T [K]	173	173	173	100	173	173
$d_{calcd.}$ [g cm^{-3}]	3.380	3.607	2.727	2.161	2.659	2.598
λ [Å]	0.71073	0.71073	0.71073	0.49594	0.71073	0.71073
min/max θ [°]	2.36/28.18	2.53/28.15	1.93/28.11	2.96/22.42	1.92/28.19	1.98/27.46
Final R_1[a] [$I > 2\sigma(I)$]	0.0348	0.0358	0.0362	0.0423	0.0269	0.0423
Final wR_2[b] [$I > 2\sigma(I)$]	0.0685	0.0880	0.0685	0.1096	0.0547	0.1055
GOF	1.068	1.337	1.252	1.094	1.249	1.183

[a] $R_1 = \Sigma||F_o| - |F_c||/|F_o|$. [b] $wR_2 = \{\Sigma[w(F_o^2 - F_c^2)^2]/\Sigma[w(F_o^2)^2]\}^{0.5}$.

0.60 g sample of $Na_4K_2[Nb_4W_2O_{19}]\cdot 12H_2O$ (0.42 mmol) dissolved in 10 mL of H_2O by heating to ~60 °C and stirring. The solution was then heated to ~95 °C and stirred until the volume was reduced by ~70%. The solution was slowly cooled to room temperature, and after several minutes crystals began to form. After 1–3 d, 0.57 g (80% yield) of purple plate-like crystals was collected by suction filtration, washed with methanol, and dried in vacuo. IR (ATR, 1100–400 cm^{-1}): $\tilde{\nu}_{max}$ = 1031 (m), ~901 (sh), 846 (m), 745 (sh), 689 (s), 526 (s) cm^{-1}. $C_{12}H_{60}Cu_3N_{12}Nb_4O_{25}W_2$ (1702.6): calcd. Cu 11.2, Nb 21.8, W 21.6; found Cu 12.4, Nb 24.4, W 24.3.

Crystallographic Studies. 1, 2, 3, 5, and 6: Single-crystal X-ray diffraction was performed at 173 K with a Bruker AXS SMART-CCD diffractometer with graphite-monochromated Mo-K_α (0.71073 Å) radiation. Data collection and reduction were carried out with SMART 5.054 (Bruker, 1998)[47] and SAINT 6.02 (Bruker, 2001)[48] software, respectively. An empirical absorption correction was applied using SADABS 2.05.[49] All subsequent structure solution and refinement were performed within the WinGX[50] system. The structure was solved by Direct Methods (program SIR97[51]) and refined by full-matrix least squares on F^2 (SHELX97[52]). **4:** Since crystals of **4** were too small for conventional single-crystal X-ray diffraction, the data for **4** was collected with a 15-ID ChemMatCARS beamline equipped with a Bruker 6000 CCD detector at Advanced Photon Source, Argonne National Laboratory. The data were collected at 100 K with radiation of 0.49594 Å wavelength, an exposure time of 1 s per frame, and a detector distance of 5.0 cm. Data were collected down to a resolution of 0.5527 Å^{-1}. The raw intensity data were collected and integrated with software packages SMART 5.054 (Bruker, 1998)[50] and SAINT 6.02 (Bruker, 2001)[48]. An empirical absorption correction was applied using SADABS.[49] The crystal structure was solved by Direct Methods and refined assuming anisotropical displacement parameters for all atoms with SHELX97.[52] The crystallographic data for the six structures are summarized in Table 3, and further details of **2** may be obtained from the Fachinformationszentrum Karlsruhe, 76344 Eggenstein-Leopoldshafen, Germany on quoting depository number CSD-419429. CCDC-685804 (**1**), -685805 (**3**), -685806 (**4**), -685807 (**5**), and -685808 (**6**) contain the additional supplementary data for this paper. These data can be obtained free of charge from The Cambridge Crystallographic Data Centre via www.ccdc.cam.ac.uk/data_request/cif.

Acknowledgments

The Sandia authors thank the Sandia National Laboratories' Laboratory Directed Research and Development (LDRD) program for funding, and J. B. P. and W. X. acknowledge support from the NSF through Grant DMR-0800415. Sandia is a multiprogram laboratory operated by the Sandia Corp., a Lockheed Martin Co., for the U. S. DOE's National Nuclear Security Administration under Contract DE-AC04-94AL85000. ChemMatCARS Sector 15 is principally supported by the National Science Foundation/Department of Energy under Grant CHE-0087817. The Advanced Photon Source is supported by the U.S. Department of Energy, Basic Energy Sciences, Office of Science, under Contract No. W-31-109-Eng-38.

---

[1] I. Lindqvist, *Ark. Kemi* **1953**, *5*, 247–250.
[2] M. T. Pope, B. W. Dale, *Q. Rev. Chem. Soc.* **1968**, *22*, 527–549.
[3] M. Muller, *Rev. Chim. Miner.* **1970**, *7*, 359–411.
[4] M. T. Pope, *Heteropoly and Isopoly Oxometalates*, Springer-Verlag, Berlin, **1983**.
[5] M. T. Pope in *Comprehensive Coordination Chemistry II: From Biology to Nanotechnology*, vol. 4 (Ed.: A. G. Wedd), Elsevier Ltd., Oxford, UK, **2004**, pp. 635–678.
[6] B. W. Dale, M. T. Pope, *Chem. Commun. (London)* **1967**, 792.
[7] C. M. Flynn Jr, G. D. Stucky, *Inorg. Chem.* **1969**, *8*, 178–180.
[8] C. M. Flynn Jr, G. D. Stucky, *Inorg. Chem.* **1969**, *8*, 332–334.
[9] C. M. Flynn Jr, G. D. Stucky, *Inorg. Chem.* **1969**, *8*, 335–344.
[10] B. W. Dale, J. M. Buckley, M. T. Pope, *J. Chem. Soc. A* **1969**, 301–304.
[11] A. Goiffon, E. Philippot, M. Maurin, *Rev. Chim. Miner.* **1980**, *17*, 466–476.
[12] T. Ozeki, T. Yamase, H. Naruke, Y. Sasaki, *Bull. Chem. Soc. Jpn.* **1994**, *67*, 3249–3253.
[13] A. V. Besserguenev, M. H. Dickman, M. T. Pope, *Inorg. Chem.* **2001**, *40*, 2582–2586.
[14] K. Hegetschweiler, R. C. Finn, R. S. Rarig Jr, J. Sander, S. Steinhauser, M. Worle, J. Zubieta, *Inorg. Chim. Acta* **2002**, *337*, 39–47.
[15] T. M. Alam, M. Nyman, B. R. Cherry, J. M. Segall, L. E. Lybarger, *J. Am. Chem. Soc.* **2004**, *126*, 5610–5620.
[16] M. Nyman, T. M. Alam, F. Bonhomme, M. A. Rodriguez, C. S. Frazer, M. E. Welk, *J. Cluster Sci.* **2006**, *17*, 197–219.

[17] D. Laurencin, R. Thouvenot, K. Boubekeur, A. Proust, *Dalton Trans.* **2007**, 1334–1345.

[18] R. P. Bontchev, E. L. Venturini, M. Nyman, *Inorg. Chem.* **2007**, *46*, 4483–4491.

[19] J.-P. Wang, H.-Y. Niu, J.-Y. Niu, *Inorg. Chem. Commun.* **2008**, *11*, 63–65.

[20] T. Ozeki, T. Yamase, H. Naruke, Y. Sasaki, *Inorg. Chem.* **1994**, *33*, 409–410.

[21] H. Naruke, T. Yamase, *J. Alloys Compd.* **1997**, *255*, 183–189.

[22] T. M. Anderson, S. G. Thoma, F. Bonhomme, M. A. Rodriguez, H. Park, J. B. Parise, T. M. Alam, J. P. Larentzos, M. Nyman, *Cryst. Growth Des.* **2007**, *7*, 719–723.

[23] R. Haugsrud, T. Norby, *Nat. Mater.* **2006**, *5*, 193–196.

[24] Y. Kawakami, H. Ikuta, M. Wakihara, *J. Solid State Electrochem.* **1998**, *2*, 206–210.

[25] V. Thangadurai, S. Adams, W. Weppner, *Chem. Mater.* **2004**, *16*, 2998–3006.

[26] K. Tanabe, S. Okazaki, *Appl. Catal., A* **1995**, *133*, 191–218.

[27] I. Nowak, M. Ziolek, *Chem. Rev.* **1999**, *99*, 3603–3624.

[28] M. Ziolek, *Catal. Today* **2003**, *78*, 47–64.

[29] N. Ballarini, G. Calestani, R. Catani, F. Cavani, U. Cornaro, C. Cortelli, M. Ferrari, *Stud. Surf. Sci. Catal.* **2005**, *155*, 81–94.

[30] L. Tsonev, *Opt. Mater.* **2008**, *30*, 892–899.

[31] M. Dabbabi, M. Boyer, *J. Inorg. Nucl. Chem.* **1976**, *38*, 1011–1014.

[32] C. Rocchiccioli-Deltcheff, R. Thouvenot, M. Dabbabi, *Spectrochim. Acta Part A* **1977**, *33*, 143–153.

[33] M. Dabbabi, M. Boyer, J. P. Launay, Y. Jeannin, *J. Electroanal. Chem.* **1977**, *76*, 153–164.

[34] C. J. Besecker, W. G. Klemperer, *J. Am. Chem. Soc.* **1980**, *102*, 7598–7600.

[35] C. J. Besecker, V. W. Day, W. G. Klemperer, M. R. Thompson, *J. Am. Chem. Soc.* **1984**, *106*, 4125–4136.

[36] R. P. Bontchev, M. Nyman, *Angew. Chem. Int. Ed.* **2006**, *45*, 6670–6672.

[37] J. Niu, P. Ma, H. Niu, J. Li, J. Zhao, Y. Song, J. Wang, *Chem. Eur. J.* **2007**, *13*, 8739–8748.

[38] E. J. Graeber, B. Morosin, *Acta Crystallgr.* **1977**, *B33*, 2137–2143.

[39] K. A. Marek, PhD thesis, University of Illinois at Urbana–Champaign, **2001**.

[40] M. R. Antonio, unpublished results.

[41] J. M. Machefert, A. D'Huysser, M. Lenglet, J. Lopitaux, D. Delahaye, *Mat. Res. Bull.* **1988**, *23*, 1379–1388.

[42] B. M. Weckhuysen, R. A. Schoonheydt, *Catal. Today* **1999**, *49*, 441–451.

[43] A. Galli, G. Poldi, M. Martini, E. Sibilia, *Phys. Status Solidi* **2007**, *4*, 950–953.

[44] C. J. Besecker, W. G. Klemperer, V. W. Day, *J. Am. Chem. Soc.* **1982**, *104*, 6158–6159.

[45] Y. Komiyama, E. C. Lingafelter, *Acta Crystallogr.* **1964**, *17*, 1145.

[46] V. Manriquez, M. Campos-Vallette, N. Lara, N. Gonzalez-Tejeda, O. Wittke, G. Diaz, S. Diez, R. Munoz, L. J. Kriskovic, *J. Chem. Crystallogr.* **1996**, *26*, 15–22.

[47] *SMART*, version 5.054, Bruker AXS, Inc., Madison, WI, **1998**.

[48] *SAINT*, version 6.02, Bruker AXS, Inc. Madison, WI, **2001**.

[49] G. M. Sheldrick, *SADABS*, version 2.10, University of Göttingen, Göttingen, Germany, **2003**.

[50] L. J. Farrugia, *J. Appl. Crystallogr.* **1999**, *32*, 837–838.

[51] A. Altomare, M. C. Burla, M. Camalli, G. L. Cascarano, C. Giacovazzo, A. Guagliardi, A. G. G. Moliterni, G. Polidori, R. Spagna, *J. Appl. Crystallogr.* **1999**, *32*, 115–119.

[52] *SHELX97*, Programs for Crystal Structure Analysis, release 97-2, Institut für Anorganische Chemie der Universität, Göttingen, Germany, **1998**.

Received: April 23, 2008